THE JOURNAL OF PHYSICAL CHEMISTRY A

A: Spectroscopy, Molecular Structure, and Quantum Chemistry

Photochemistry of the Stilbenes in Methanol. Trapping the Common Phantom Singlet State

Jack Saltiel, and Shipra Gupta

J. Phys. Chem. A, **Just Accepted Manuscript** • DOI: 10.1021/acs.jpca.8b04011 • Publication Date (Web): 21 Jun 2018

Photochemistry of the Stilbenes in Methanol. Trapping the Common Phantom Singlet State

Jack Saltiel, and Shipra Gupta*

Department of Chemistry and Biochemistry, Florida State University, Tallahassee, FL 32306-4390

Corresponding Author

*saltiel@chem.fsu.edu

ABSTRACT: A comparative study of the photochemistry of *cis*- and *trans*-stilbene in methanol shows that both isomers undergo methanol photoaddition giving similar yields of α-methoxybibenzyl in competition with cis-trans photoisomerization. Methanol addition occurs primarily following torsional relaxation of the lowest excited singlet states of each isomer, $^1c^*$ and $^1t^*$, to a common twisted singlet excited state intermediate, $^1p^*$, initially called the phantom singlet state. The addition is consistent with the zwitterionic character of $^1p^*$. Ether forms by direct 1,2-addition of CH_3OH to the central carbon atoms and by 1,1-addition following rearrangement to 1-benzyl-1-phenylcarbene. Use of CD_3OD and GC/MS (gas chromatographic/mass spectroscopic) analysis of the ether products revealed that the ratio of carbene/direct addition pathways is higher starting from *cis*-stilbene. We conclude that $^1p^*$ formed from $^1c^*$ is hotter than $^1p^*$ formed from $^1t^*$. Surprisingly, except for favoring the carbene pathway, the use of higher energy photons (254

vs 313 nm) does not affect the overall ether quantum yield starting from *cis*-stilbene, but significantly enhances both pathways starting from *trans*-stilbene. It appears that carbene formation and direct methanol addition to higher *trans*-stilbene excited state(s) compete with relaxation to S_1. Substitution of D for the vinyl Hs of stilbene enhances the direct addition pathway more than two-fold and strongly suppresses the carbene insertion pathway, revealing a large, k_{pc}^{d0}/k_{pe}^{d2} = 6.3, primary deuterium isotope effect in the carbene rearrangement. The two-fold increase in the ether quantum yield is due primarily to a 2.75-fold increase in the lifetime of $^1p^*$ on deuterium substitution of the vinyl hydrogens.

INTRODUCTION

Extensively studied, the stilbenes serve as the prototypical example of molecules undergoing cis-trans photoisomerization.[1-3] They have played a central role in studies of the effect of solvent friction on S_1 torsional relaxation, the initial step in isomer interconversion.[2,3] In hydrocarbon solvents, torsional relaxation from the trans side, the major process competing with fluorescence at all temperatures (*T*s),[1] is subject to an energy barrier that is in part intrinsic, 2.9 kcal/mol, and in part diffusional, 0.4 E_η, where E_η is the activation energy of viscous flow.[4-6] Torsional relaxation from the cis side is entirely diffusional and subject to most, if not all, of E_η.[7] Both isomers give a twisted intermediate $^1p^*$, initially named the phantom excited singlet state in anticipation of its fleeting existence.[8,9] Decay from $^1p^*$ slightly favors *cis*-stilbene, ^1c, over *trans*-stilbene, ^1t, and there is a reverse torsional component from $^1p^*$ to $^1t^*$ that is responsible for a minor adiabatic $^1c^* \rightarrow {}^1t^*$ reaction channel.[7,10,11] Conrotatory cyclization to 4a,4b-dihydrophenanthrene, DHP, is a competing $^1c^*$ reaction, less prominent than cis-trans photoisomerization.[12-15] Ether formation was reported as a minor reaction channel on irradiation

of ^1t in methanol[16] (MeOH) or 2,2,2-trifluoroethanol[17,18] (TFE). In the case of TFE, of the mechanisms considered for the direct alcohol reaction with excited stilbene, protonation of $^1t^*$ was favored.[17,18]

We recently described our work on the mechanism of ether formation resulting from the irradiation of the three 1,4-diphenyl-1.3-butadiene (DPB) isomers in ethanol.[19] The key excited state that reacted with the alcohol was proposed to be a twisted zwitterionic *trans*-phenallyl cation/benzyl anion formed efficiently from *trans,trans*- and *cis,trans*-1,4-diphenyl-1.3-butadiene and inefficiently from *cis,cis*-1,4-diphenyl-1.3-butadiene.[19] A reevaluation of the stilbene results led us to propose that alcohol addition to a zwitterionic twisted phantom singlet state is a more likely path to ether.[19] The results in this paper substantiate that proposal.

EXPERIMENTAL SECTION

Materials. The perhydrostilbenes, *t*- and *c*-St_{d0} and their α,α´-dideuterio derivatives, *t*- and *c*-St_{d2} were previously described.[5,11] They were purified by chromatography with hexane eluent on silica immediately before use. Methanol (Sigma Aldrich, Spectrometric Grade, Anhydrous), methanol-d_4 (Cambridge Isotopes, 10x 0.5 mL pack), hexane (HPLC grade, EMD), cyclohexane (VWR, Spectrometric Grade, anhydrous) and silica, 230-400 mesh, (Sigma-Aldrich, technical grade) were used as received.

Irradiation Procedures. Sample preparation and degassing procedures were described previously.[20] Sets of 13 mm o.d. Pyrex tubes fitted with standard taper joints and grease traps were loaded with 2.0 mL aliquots of St solutions. They were degassed using 4 freeze-pump-thaw cycles to $< 10^{-4}$ Torr and flame sealed at a constriction. All operations, including analyses, were performed under nearly complete darkness (red light). Irradiations were carried out in a Moses

merry-go-round[21] apparatus immersed in a water bath thermostated to 22.0 °C. A heating coil connected to a thermoregulator (Polyscience Corp.) was used to control the temperature to ± 0.5 °C. The photoisomerization of *t*-St in CH_3OH was used for actinometry, $\phi_{tc} = 0.54$.[22-24] Hanovia 450-W medium pressure Hg lamps were employed. The 313 nm Hg line was isolated using a potassium perchromate/potassium carbonate filter solution1[20] Irradiations in CD_3OD were carried out in N_2 outgassed ampules using 3.0 mL aliquots at 23 ±0.5 °C. Small samples, 0.3 μL, were removed periodically for GC analysis.

To conserve the deuterated solvent, 254 nm irradiations of 0.50 mL aliquots of N_2 outgassed CD_3OD solutions were carried out in capped quartz NMR tubes using a previously described cylindrical merry-go-round attached to a stirring motor.[25] The samples were placed at a distance of 3 in from the Hg lamps. A 12-W low pressure Hanovia Hg lamp inserted in a cylindrical Vycor glass sleeve was employed. Temperature was maintained in the 24.8-25.6 °C range.

Analytical Procedures. Analysis of product composition was by GC,[26] by ^{1}H NMR and, for deuterated samples, by GC/MS. A Bruker/Varian CP-3800 gas chromatograph equipped with an electronic integrator was used. Samples were concentrated to approximately 1 mL under a stream of N_2 and 0.1-0.2 μL aliquots were injected onto a Varian Factor Four column. Analyses were carried out at an initial temperature of 100 ºC that was increased to 220 ºC using a 20 ºC/min ramp. The injector inlet and the FID detector were both held at 250 ºC, and an initial injector split ratio of 30:1 was increased to 60:1 after 0.75 min and decreased to 5:1 after 1.25 more min to conserve carrier gas. A Bruker Avance III 500 MHz spectrometer was used for ^{1}H NMR spectra. GC response factors of the St isomers were assumed to be identical. The GC molar response factor of the ether photoproduct, *E*, was determined to be 0.503 relative to *t*-St by

relating the quantitative ^{1}H NMR analysis of an irradiation mixture to GC peak areas for the same mixture. This ratio of *E*/St molar response factors is in excellent agreement with 0.507, the analogous *E*/DPB ratio.[19] Accordingly, ether GC areas were multiplied by 1.98_7 before calculating % molar conversions. Reduction of FID molar response factors with introduction of heteroatoms in hydrocarbons is a known phenomenon.[27,28]

A Varian Cary 300B UV-Vis spectrophotometer was used to record absorption spectra at 20.5 °C using a thermostated cell holder.

RESULTS

Stilbene-d_0 – Methanol-d_0, 313 nm. Six pairs of sealed ampules containing degassed methanol solutions were exposed to 313 nm excitation in parallel. Ampule pairs were periodically removed from the merry-go-round for GC analysis. Initial concentrations were [*c*-St] = 0.0154 M and [*t*-St] = 0.0140 M. Isomer contaminations at 0-time, determined by GC analysis, were 0.25% *c*-St in *t*-St and 0.13% *t*-St in *c*-St. The quasi-photostationary state attained on prolonged irradiation of the same stilbene solutions, (89.6 ± 0.1)% *c*-St, is in reasonable agreement with the reported photostationary state of 91.7% *c*-St in *n*-pentane.[20] Photoisomerization conversions at time *t*, f_c^t and f_t^t starting from *t*- and *c*-St, respectively, were corrected for back reaction[29] and for initial isomer contamination,[20] f_x^0, eq 1, using the quasi-photostationary fraction of stilbene product, f_x^{eq}.

$$f_x^{corr} = f_x^{eq} \ln\left(\frac{f_x^{eq} - f_x^0}{f_x^{eq} - f_x^t}\right) \quad (1)$$

Conversions to the ether, corrected for the difference in relative ether and stilbene GC molar responses, and back reaction corrected conversions to the two stilbene isomers are linearly dependent on time, Figure 1. Photoisomerization quantum yields are given in Table S1.

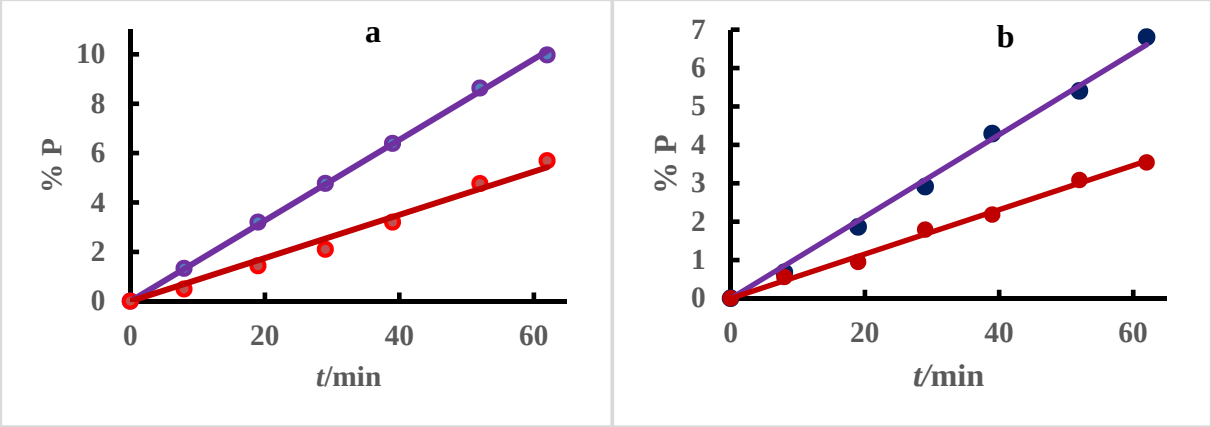

Figure 1. Conversions in CH_3OH starting from *t*- and *c*-St in panels a and b, respectively – lines are blue for St and red for ether product (P). Ether % conversions are multiplied by 10^2.

Stilbene-d_0 – Methanol-d_4, 313 nm. Aliquots, 3 mL, of stilbene solutions in CD_3OD having initial concentrations of [*c*-St] = 0.0216 M and [*t*-St] = 0.0210 M were transferred into a pair of Pyrex ampules. The ampules were outgassed with a gentle stream of N_2 gas using latex tubing and sealed with a rubber septum. They were irradiated in parallel in the merry-go-round at 313 nm at 22.5 ± 0.5 °C and the progress of the reactions was monitored by GC using no more than 0.3 μL injections. The N_2 outgassing was repeated after each injection. Prolonged irradiation under these conditions led to a quasi-PSS of 89.9% *c*-St and 10.1 % *t*-St. Isomer contaminations

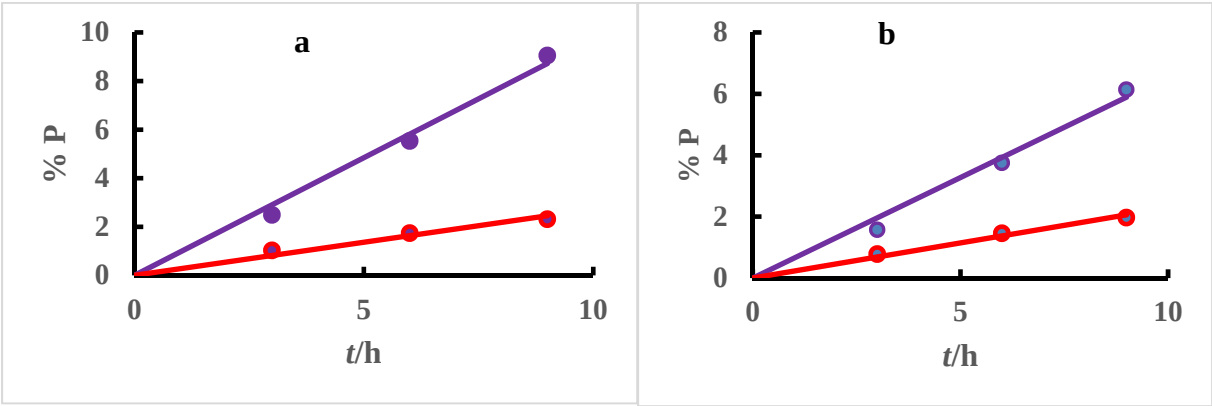

Figure 2. Conversions at 313 nm in CD_3OD starting from *t*- and *c*-St in panels a and b, respectively – lines are blue for St and red for ether. Ether % conversions are multiplied by 10^2.

at 0-time, determined by GC analysis, were 0.09% *c*-St in *t*-St and 0.39% *t*-St in *c*-St. Product conversions over an irradiation period of 9 h are plotted against irradiation time in Figure 2. Quantum yields based on the slopes of the lines in Figure 2 are given in Table S1.

Scheme 1. Ethers E_{12} and E_{11} from the Photoaddition of CD_3OD to Stilbene

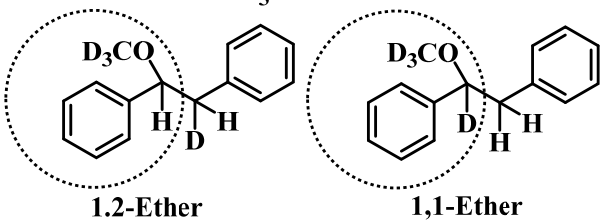

Because there is a systematic deviation of the points from the photoisomerization lines in panels a and b of Figure 2, isomer conversions in the two directions were also plotted against each other. The resulting line has a correlation coefficient $r^2 = 0.999$ and its slope, 0.676, gives $\phi_{c\rightarrow t} = 0.37_5$, in very good agreement with the value in Table S1. For the experiment in Figure 2, ratios of ether formed via carbene rearrangement leading to 1,1-addition of CD_3OD and direct 1,2-addition of CD_3OD, 0.456 and 0.678 starting from *t*- and *c*-St, respectively, were determined by GC/MS immediately after the last irradiation period. They were based on the ratios of the 125 to 124 mass base peaks after correction of the 125 peak for the expected 8.99% M + 1 contributions due to ^{13}C, ^{2}H and ^{17}O natural abundances, Scheme 1. In Scheme 1 the base peak fragments are circled. An independent experiment in which GC/MS analysis was performed after St conversions close to the PSS value and 2.1% ether yields had been achieved, the corrected 125/124 peak ratios were 0.555 and 0.529, starting from *t*- and *c*-St, respectively. The ether forming steps are shown in Scheme 2.

Scheme 2. Photoaddition of CD_3OD to the Stilbenes

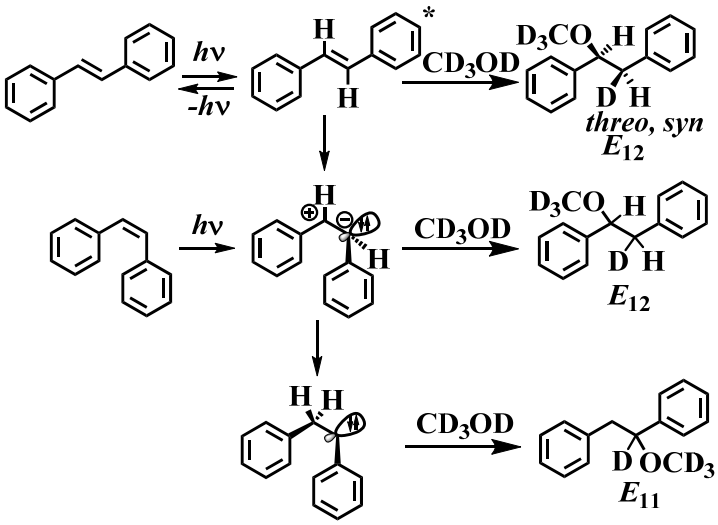

Stilbene-d_0 – Methanol-d_4, 254 nm. Aliquots, 0.50 mL, of *c*- and *t*-St solutions 0.0199 and 0.0250 M, respectively, in anhydrous methanol were delivered into two quartz NMR tubes. The methanol was completely evaporated and replaced with 0.50 mL of CD_3OD. Each tube was then outgassed with a slow stream of N_2 for 20 min to minimize solvent evaporation and capped. A 12-W low pressure Hg lamp placed in a Vycor sleeve (220 nm cutoff) was used to irradiate the samples in parallel in a merry-go-round designed for NMR tubes. The progress of the reaction was followed by GC analysis. Prolonged irradiation under these conditions led to a quasi-PSS of 47.4% *c*-St and 52.6 % *t*-St. Isomer contaminations at 0-time, determined by GC analysis, were 0.09% *c*-St in *t*-St and 0.39% *t*-St in *c*-St. Product conversions over an irradiation period of 60

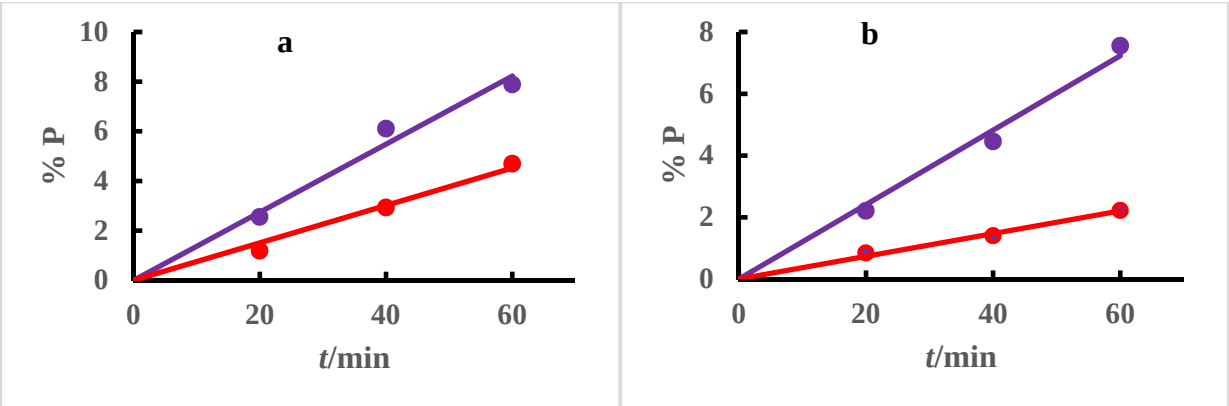

Figure 3. Conversions at 254 nm in CD_3OD starting from *t*- and *c*-St in panels a and b, respectively – lines are blue for St and red for ether. Ether % conversions are multiplied by 10^2.

min are plotted against irradiation time in Figure 3. Quantum yields based on the slopes of the lines in Figure 3 are given in Table S1. For the experiment in Figure 3, ratios of direct 1,2-addition of CD_3OD to 1,1-addition of CD_3OD via carbene rearrangement of 0.82_4 and 1.0_3 starting from *t*- and *c*-St, respectively, were again based on the corrected ratios of the 124 to 125 mass peaks determined by GC/MS after the last irradiation period. Quantum yields from an

independent experiment in which *t*-St CH_3OH solutions were irradiated without the Vycor filter sleeve are in excellent agreement with those in which the filter sleeve was employed, Table S1.

***trans*-Stilbene-*d*$_2$ – Methanol-*d*$_0$, 313 nm.** The procedure used in this experiment is identical to that described above for the 313 nm irradiation of the undeuterated stilbenes. Isomer contamination at 0-time, determined by GC analysis, was 0.12% *c*-St-d$_2$. The irradiated methanol solution was 0.0220 M *t*-St-d$_2$. Product conversions over an irradiation period of 122 min, corrected for back reaction are plotted against irradiation time in Figure 4. The quantum yield for ether formation,

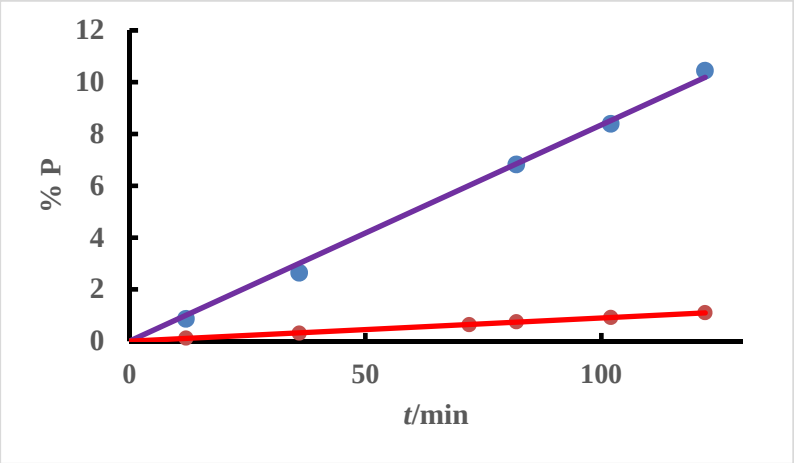

Figure 4. Conversions for the 313 nm irradiation of *t*-St-d$_2$ in CH_3OH – lines are blue for *c*-St-d$_2$ and red for ether. Ether % conversions are multiplied by 10^2.

based on the slopes of the lines in Figure 4 and the assumption that $\phi_{t\rightarrow c}$ = 0.54 is 0.0057$_9$, Table S1. The ratio of carbene insertion to direct addition pathways to ether, 0.120, was based on the GC/MS relative intensities of the 121 (via carbene insertion) and 122 (via direct addition) peaks.

DISCUSSION

Laarhoven and coworkers[16] used CH_3OD to find two significant routes to α-methoxybibenzyl: (1) direct 1,2-addition of CH_3O/D to the double bond to give threo and erythro ethers and (2) 1,1-addition of CH_3O/D via rearrangement to a carbene, followed by carbene insertion into CH_3OD. Higher energy photons were found to favor the carbene over the direct ether pathway and the threo over the erythro adduct. Two reactive states were considered, in addition to the lowest excited states, one of which is either a higher energy electronic state – Rydberg states have been proposed in carbene formation from alkenes[30] – or a vibrationally excited S_1 state involved in carbene and *threo*-ether formations. The results were deemed inconclusive as to the mechanism of ether formation by direct methanol addition. Involvement of an excited singlet zwitterionic twisted intermediate, $^1p^*$, was ruled out and addition of methanol to planar *t*- and *c*-St S_1 states, $^1t^*$ and $^1c^*$, was considered a viable mechanism because 1,2-diphenylcyclopentene, erroneously thought to have an obligatory planar excited state,[31] also undergoes the reaction. Syn additions of CH_3OD to $^1t^*$ and $^1c^*$ were proposed as routes to threo and erythro ethers, respectively.[24] The possibility of addition to a biradical $^1p^*$ was also considered. What was overlooked is that irradiation of *t*-St in methanol at 300 nm leads to continuous unabated ether formation as a cis rich (~ 85% *c*-St) quasi-photostationary state is quickly approached and maintained (see Figure 1 in ref 24). Formation of the ethers at an almost constant rate, independent of stilbene isomer composition, indicates that the ethers form from the two isomers with very similar efficiencies.

The photoaddition of 2,2,2-trifluoroethanol (TFE) to stilbene was reported, subsequently, by Roberts and Pincock.[17,18] In the more acidic TFE, St was found to give ether photoadduct faster than in methanol.[17] Use of TFE-OD established that, due to faster protonation, the carbene pathway to ether is less important than in CH_3OH.[18] The fluorescence of methoxy-substituted

trans-stilbenes is quenched by TFE in acetonitrile, and formation of cation intermediates was observed by pulsed laser excitation.[18] Protonation of S_1 followed by nucleophilic attack on the resulting cation was assumed to apply also to the parent *t*-St. However, here too, the fact that the rate of ether formation was found to be independent of *cis/trans* St composition,[17] points to $^1p^*$ as a common reactive stilbene intermediate. To the extent that the initial S_1 states of the stilbene isomers are involved in ether formation, one would expect $^1t^*$ to play a more prominent role than $^1c^*$ because the lifetime of $^1t^*$ in CH_3OH, 43 ps at 297 K,[32,33] is almost 10^2 times longer than the lifetime of $^1c^*$, 0.48±0.02 ps under similar conditions.[34-39] It was proposed that the shorter stilbene S_1 lifetimes in more polar solvents generally, and in methanol specifically, were due to the lowering of the energy of the potential energy surface along torsional coordinates leading to a relatively polar $^1p^*$.[23.24] This is not easily established because experimental Arrhenius activation energies for torsional relaxation in solution involve coupled solvent/solute dynamics and do not readily reveal solute-specific properties. We had shown that experimental activation enthalpies, ΔH_{obsd}, in the *n*-alkane family depend linearly on E_η, the activation energy for viscous flow.[4,5] They can be calculated by adding 0.4 E_η to 2.9 kcal/mol, the intrinsic energy barrier for torsional relaxation.[4,5] In changing the solvent from hexane[4] to methanol[32,33] the activation energy for the $^1t^* \rightarrow {}^1p^*$ process increases from 4.1 to 4.6 kcal/mol (the value of the Arrhenius activation energy in hexane is the activation enthalpy[4] plus 0.6 kcal/mol for *RT*). The activation energy for the $^1t^* \rightarrow {}^1p^*$ process in methanol is anomalously high compared to higher members of the *n*-alcohol series where the linear ΔH_{obsd} vs E_η relationship is not obeyed.[2] The short $^1t^*$ lifetimes in methanol are due to compensation of the larger activation energies by even larger pre-exponential factors. The corresponding effective activation energy change on changing the solvent for the $^1c^* \rightarrow {}^1p^*$ process from hexane to methanol is not known. However, it has been

shown that in hydrocarbon solvents that process experiences no intrinsic barrier.[7] It occurs as a diffusion controlled process, subject to almost the entire activation energy of viscous flow.[7] No such simple relationship exists in alcohols where stronger specific solute/solvent and solvent/solvent hydrogen bonding interactions are involved whose disruption as the molecule proceeds to a zwitterionic $^1p^*$ probably fail to keep up with the molecular motion of the solute. Solvent reorganization contributes significantly to the activation enthalpies and entropies of torsional relaxation, especially in the much faster $^1c^* \rightarrow {}^1p^*$ direction. Torsional barriers starting from $^1t^*$ and $^1c^*$ have also been estimated from isoviscosity Arrhenius plots.[38,40] They are of dubious physical significance, not least of all, because of their reliance on sheer viscosity, a macroscopic property, as a measure of solvent friction.[2,4-6] At least in the family of *n*-alkanes, torsional rate constants are much better behaved when microviscosities based on empirical solute diffusion coefficients are employed instead of sheer viscosity.[4-6] However, there is no reason to expect microfriction approaches to work with alcohols. Fleming and coworkers, Waldeck and coworkers and others have discussed these issues in greater detail.[3] There is ample evidence that in the gas phase the OH proton of methanol hydrogen bonds to the π electron cloud of benzene.[41,42] But as the number of methanol molecules in the complex increases the nature of the interaction with benzene changes as methanol molecules hydrogen bond more strongly to each other than to benzene. Similar hydrogen bonding should also involve the phenyl groups of stilbene. To account for the methanol solvent effect in solution one would have to know how hydrogen bonding interactions change as each excited stilbene isomer undergoes torsional motion over a polar/polarizable transition state to a zwitterionic $^1p^*$.

The $^1p^*$ intermediate. Early *c*-St transient absorption studies assigned a broad spectrum to $^1c^*$ with $\lambda_{max} \sim 700$ nm whose decay, $\tau_c = 1.0$ ps in hexane, gives rise to a transient with $\lambda_{max} \sim 335$

nm that was attributed to hot *t*-St product.[34] An upper limit of 0.15 ps was estimated for the lifetime, τ_p, of $^1p^*$.[34] Our estimates of τ_p of 0.21 to 0.26 ps in hexane[7] were based on steady state measurements of the efficiency of the adiabatic $^1c^* \rightarrow {}^1p^* \rightarrow {}^1t^*$ channel.[7,10,11] A *c*-St transient absorption study[43] employed more sophisticated instrumentation to refine and extend the initial transient observations.[34-37] In hexane, the $^1c^*$ transient, λ_{max} = 635 nm, was observed to decay to the 335 nm transient, now assigned to $^1p^*$, which subsequently decays to hot ground state $^1c/^1t$ product whose cooling leads to sharpening of the absorption band. Two kinetics models were employed to account for the time evolution of the transients. The authors expressed preference for the model in which the $^1c^*$ to $^1p^*$ conversion is reversible over the usual model of sequential irreversible $^1c^* \rightarrow {}^1p^* \rightarrow {}^1p$ steps.[43] Use of the reversible kinetics model gives τ_p = 0.33 ps in hexane at room temperature.[43] But, this reversibility model can be discarded because, assuming a common $^1p^*$ intermediate, reversibility requires that excitation of *t*-St give measurable amounts of dihydrophenanthrene, DHP, in contradiction to steady state observations that established long ago that DHP[44] forms exclusively from *c*-St.[45-47] The induction period in the time evolution of the DHP photoproduct in methanol starting from *t*-St[16] demonstrates the obligatory excitation of *c*-St in DHP formation. Assuming irreversible formation of $^1p^*$ gives τ_p = 0.23 ps in excellent agreement with our estimate of τ_p.[7] The biexponential decay model was also used by the authors in a more recent publication.[48] Observation of DHP absorption following *t*-St excitation and the absence of $^1t^*$ transient absorption following *c*-St excitation again led to the conclusion that $^1t^* \rightarrow {}^1p^* \rightarrow {}^1c^*$ adiabatic isomerization occurs in hexane, whereas the reverse adiabatic pathway $^1c^* \rightarrow {}^1p^* \rightarrow {}^1t^*$ does not.[48] The authors did not consider that, based on our steady state fluorescence observations,[7] only 0.3% of the molecules that reach $^1p^*$ give $^1t^*$ and such a small yield would be undetectable in transient absorption. The observation of DHP following ^1t

excitation (Fig. 16 in ref 48) may be due to excitation of photoproduct ^1c in the laser beam path by a second photon.

A recent study found biexponential $^1c^*$ fluorescence decay in cyclohexane with τ_c = 1.2 ps and τ_c' = 0.23 ps and assigned the 0.23 ps process to the initial partitioning between photoisomerization and photocyclization pathways from $^1c^{*\prime}$, an early excited state, and the 1.2 ps process to the subsequent $^1c^*$ that undergoes torsional relaxation along the photoisomerization pathway.[49] Although resolved fluorescence spectra associated with the two components are very similar, it was proposed that they originate from significantly different $^1c^{*\prime}$ and $^1c^*$ geometries on an energetically flat potential energy surface. However, geometries of excited *c*-St that differ in the degree of planarity would be expected to have different fluorescence spectra and if they lay on an energetically flat potential energy surface should be present as an equilibrium mixture. Decay to and from an equilibrium mixture involving two $^1c^*$conformers, one poised for torsional relaxation and the other poised for cyclization to DHP, could account for biexponential $^1c^*$ fluorescence and transient absorption decays.

The Kinetics of Ether Formation. The results in Table S1 are generally consistent with the observations of Laarhoven and coworkers,[16] but their more quantitative nature reveals hitherto hidden mechanistic details. The observation of similar ether quantum yields from *t*- and *c*-St is most important because it implicates $^1p^*$ as the major ether precursor by direct methanol 1,2-addition and by 1,1-adition following $^1p^*$ rearrangement to a carbene. As reported by Laarhoven and coworkers,[16] higher energy photons give higher ether yields. If the higher energy pathway to ether involved formation of hot $^1p^*$, it would be more likely to originate from $^1c^*$ because, absent an intrinsic torsional barrier, the $^1c^* \rightarrow {}^1p^*$ process is faster than the activated $^1t^* \rightarrow {}^1p^*$ process.

The larger contribution of the carbene pathway to ether on 313 nm excitation of *c*-St in CD_3OD is consistent with this expectation. We were surprised, therefore, to find that the enhanced ether yield at 254 nm is due entirely to excitation of *t*-St. It appears that there is a pathway to ethers that involves direct methanol addition and carbene formation via a higher excited state of ^1t. Whether these reactions occur in the initial transoid higher excited state, $^1t^{*\prime}$, or following $^1t^{*\prime} \rightarrow {}^1p^{*\prime}$ torsional relaxation of this state to a higher energy twisted intermediate, $^1p^{*\prime}$, remains to be established. In addition to insertion to methanol, Laarhoven and coworkers established that the carbene undergoes rearrangement back to ground state stilbenes.[16]

Zwitterionic twisted intermediates, first proposed by Dauben and coworkers to explain the stereospecific photocyclization of *trans*-3-ethylidenecyclooctene[50] and the photoaddition of methanol to 1,3-dienes,[51,52] found initial theoretical support in Salem's sudden polarization close to orthogonal olefin geometries.[53] The zwitterionic nature of $^1p^*$, the twisted stilbene conical intersection, CI,[54-57] is supported by recent theoretical calculations that predict decay through a CI attained in the ^1B_u S_1 state by central bond twisting along with pyramidalization of one of the benzylic moieties.[58-62] There is also ample experimental evidence for the involvement of zwitterionic twisted intermediates in the photoisomerizations of 1,3-dienes,[63] 1,2-diarylethenes,[64] 1,4-diphenylbutadiene[19] and 1,6-diphenylhexatriene.[65,66] Laarhoven and coworkers suggested the possibility that the rearrangement of $^1p^*$ to the carbene involves a vibrationally hot diradical intermediate.[16] Hydride shift in a zwitterionic $^1p^*$ provides a more attractive pathway, Scheme 3.

Scheme 3. The Rearrangement of $^1p^*$ to Carbene

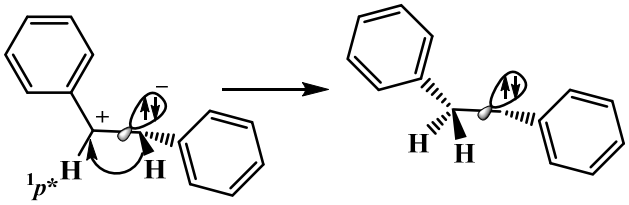

The well-established stilbene photoisomerization mechanism is augmented in eqs 2 – 16 to account for carbene and ether formation,

$$^1t + h\nu' \rightarrow {}^1t^{*\prime} \quad (2)$$

$$^1t + h\nu \rightarrow {}^1t^* \quad (3)$$

$$^1t^{*\prime} \rightarrow {}^1t^* \quad (4)$$

$$^1t^* \rightarrow {}^1t + h\nu \quad (5)$$

$$^1t^* \rightarrow {}^1p^* \quad (6)$$

$$^1p^* \rightarrow \alpha\,{}^1t + (1 - \alpha)\,{}^1c \quad (7)$$

$$^1c + h\nu \rightarrow {}^1c^* \quad (8)$$

$$^1c^* \rightarrow {}^1p^* \quad (9)$$

$$^1c^* \rightarrow \mathrm{DHP} \quad (10)$$

$$^1p^* + \mathrm{MeOH} \rightarrow E_{12} \quad (11)$$

$$^1p^* \rightarrow {}^1Carb \quad (12)$$

$$^1Carb + \mathrm{MeOH} \rightarrow E_{11} \quad (13)$$

$$^1Carb \rightarrow {}^1t + {}^1c \rightarrow \mathrm{P} \quad (14)$$

$$^1t^{*\prime} + \mathrm{MeOH} \rightarrow E_{12} \quad (15)$$

$$^1t^{*\prime} \rightarrow {}^1Carb \quad (16)$$

where α is the fraction of twisted excited singlets that decays to ^1t and k_{tt}, k_f, k_{tp}, k_d, k_{cp}, k_{cDHP}, k_{pe}, k_{pc}, k_{ec}, k_{cr}, $k_{t'd}$ and $k_{t'c}$ are the rate constants assigned to eqs 4 - 16, respectively. All the rate constants are unimolecular except for k_{pe} and $k_{t'd}$ the rate constants for methanol 1,2-addition to $^1p^*$ and $^1t^*$, respectively, which are pseudo-unimolecular. DHP stands for dihydrophenanthrene, E_{12} and E_{11}, designate ether product formed by direct 1,2-addition and by 1,1-carbene insertion, respectively, and ^1Carb stands for singlet 1-benzyl-1-phenylcarbene. P stands for phenanthrene formed from ^1Carb via the sequence of 1,2-hydride shift to the stilbenes, photochemical conversion of *c*-St to DHP and oxidation of the latter (see below). DHP forms from $^1c^*$ only, eq

10. Omitted steps from the above mechanism are $^1c^*$ fluorescence and the adiabatic $^1p^* \rightarrow {}^1t^*$ conversion. The low quantum yields of those steps, $\phi_{fc} \sim 10^{-4}$ and $\phi_{c^*t^*} \sim 0.002$, in hexane,[7,10,11] that are likely to be even smaller in the more polar methanol solvent, renders them negligible within the accuracy of our GC measurements. By eq 16 we do not wish to imply that the higher *t*-St excited state goes directly to carbene. It may do so via a higher electronic or vibrational ^1p state.

Application of the steady state approximation on all excited species gives:

$$\varphi_{tc} = (1-\alpha)k_{tp}\tau_f \tag{17}$$

$$\varphi_{ct} = \alpha k_{cp}\tau_c \tag{18}$$

$$\left(\frac{[t]}{[c]}\right)_S = \frac{\varepsilon_c}{\varepsilon_t} \times \frac{\varphi_{ct}}{\varphi_{tc}} \tag{19}$$

where ϕ_{tc} and ϕ_{ct}, are the photoisomerization quantum yields in the *trans* → *cis* and *cis* → *trans* directions, respectively, α is the fraction of twisted intermediates, $^1p^*$, that gives *t*-St, τ_f is $(k_f + k_{tp})^{-1}$, the fluorescence lifetime of $^1t^*$, and τ_c is $(k_{cDHP} + k_{cp})^{-1}$, the lifetime of $^1c^*$. Strictly speaking, the right sides of eqs 17 and 18 should be multiplied by $k_d/(k_d + k_{pc} + k_{pe})$, the fraction of $^1p^*$ that decays to the stilbenes. That fraction is too close to unity for its use to be justified. Examination of the quantum yields in Table S1 shows that use of $\phi_{tc} = 0.54$ for actinometry gives $\phi_{ct} = 0.38$ for both 313 and 254 nm excitation, in agreement with previous photoisomerization quantum yield measurements in methanol: $\phi_{tc} = 0.54 \pm 0.05$[24]and $\phi_{ct} = 0.38 \pm 0.02$.[23] Those values are about 8% higher than values in hydrocarbon solvents,[20,22.45] due to more rapid torsional relaxation in methanol,[23,24] consistent with the observation of the shorter $^1t^*$ and $^1c^*$ lifetimes. The radiative rate constants, k_f, in hexane, 6.3 x 10^8 s^{-1}, is known[5] and its value in

methanol 6.0 x 10^8 s^{-1}, can be estimated using the empirical relationship $k_f = 3.75 \times 10^8 n^{1.65}$, where 3.75 x 10^8 s^{-1} is the radiative decay of $^1t^*$ under isolated conditions and n is the refractive index of the solvent.[5] The decrease in τ_f from 76 to 43 ps[32] at 24 °C, should lead to a similar decrease in ϕ_f from 0.047 in hexane[5] to 0.026 in methanol. Since, to a very good approximation, $k_{tp}\tau_f = 1 - \phi_f$, $\alpha = 0.45$ can be calculated using eq 17. Use of eq 18 and $\phi_{ct} = 0.38$ then leads to the conclusion that 84.4% of $^1c^*$ undergo torsional relaxation and the remaining 15.6% decay via the DHP channel. A 70%/30% torsional/DHP channel split was proposed for $^1c^*$ decay in hydrocarbon media.[67,68] This was probably based on the lower $\phi_{ct} = 0.35$[20,63] in hydrocarbon solvents and the usual assumption that $\alpha = 0.5$.[68] Use of $\phi_{tc} = 0.50$ and $\phi_f = 0.047$ gives $\alpha = 0.47_5$ in hexane, the procedure we applied for the results in methanol gives a 74%/26% torsional/DHP channel split in hexane. The observed decrease of the DHP quantum yield from 0.15_5 in hexane to 0.07_7 in methanol[23] is in excellent agreement with the attenuation of the DHP decay channel. Since $^1c^* \rightarrow {}^1$DHP* is the process that competes with torsional relaxation to $^1p^*$,[37,68] about half the $^1c^*$ molecules that reach ^{1}DHP* give ground state DHP instead of one third as previously proposed.[7,69]

Similar small ether quantum yields of 0.0029 and 0.0020 from *t*- and *c*-St, respectively, are consistent with the involvement of $^1p^*$ in ether formation. They represent the sum of ether formed by direct addition of methanol to $^1p^*$ and carbene insertion in methanol. The contributions of the two pathways will be considered below. The conclusion that the lowest excited state of *t*-St, $^1t^*$, does not react with methanol validates previous interpretations of fluorescence lifetimes that consider torsional relaxation as the sole competing radiationless channel in alcohols.[3,4,24,33,40]

The Common $^1p^*$ Intermediate. Use of CD_3OD as solvent allowed separation of ether quantum yields from *t*- and *c*-St, ϕ_{te} and ϕ_{ce}, respectively, into contributions of ether formed by direct methanol addition, ϕ_{te}^d and ϕ_{ce}^d, and of ether formed via carbene insertion, ϕ_{te}^c and ϕ_{ce}^c, Table S1. For a truly common intermediate, the ratio of the two ether forming paths should be identical starting from either isomer. The fact that the carbene insertion product is favored more starting from *c-St*, does suggest that at 313 nm the $^1p^*$ that forms from $^1c^*$ is initially vibrationally hot and more prone to rearrangement.

Applying the steady state approximation to all reactive species, the mechanism in eqs 2-16 gives

$$\varphi_{ce}^{d} = k_{cp}\tau_c k_{pe}\tau_p \tag{20}$$

$$\varphi_{ce}^{c} = k_{cp}\tau_c k_{pc}\tau_p k_{ec}\tau_{carb} \tag{21}$$

$$\varphi_{te}^{d} = k_{tp}\tau_t k_{pe}\tau_p + k_{t'e}\tau_{t'} \tag{22}$$

$$\varphi_{te}^{c} = k_{tp}\tau_t k_{pc}\tau_p k_{ec}\tau_{carb} + k_{t'c}\tau_{t'} k_{ec}\tau_{carb} \tag{23}$$

where τ_c, τ_t and τ_{carb} are the lifetimes of $^1c^*$, $^1t^*$ and the carbene. The two ether pathways cannot be distinguished when CH_3OH is the solvent and observed ether quantum yields are the sum of eqs 20 and 21 for *c*-St and the sum of eqs 22 and 23 for *t*-St. With λ_{exc} = 313 nm, the results of the first experiment in Table S1 give indistinguishable ether/isomerization quantum yield ratios of 0.0054 and 0.0055 starting from *t*- and *c*-St, respectively. This would be expected if $^1p^*$ were the common ether precursor and if the partitioning fraction, α, were equal to 0.5. Our derived value of α = 0.45 indicates that those ether/isomerization ratios should differ by about 18%, $(\phi_{te}/\phi_{tc})/(\phi_{ce}/\phi_{ct}) = \alpha/(1-\alpha) = 0.82$. In view of the experimental uncertainty in our ether yields and

the small deviation of this quantity from unity, the results of the first experiment in Table S1 are consistent with the conclusion that with low energy photons $^1p^*$ and its carbene rearrangement product are the sole ether precursors. We can rule out the possibility that the $^1t^{*\prime}$ pathway, eqs 2, 15, 16, contributes to ether formation at 313 nm because that would increase ϕ_{te} and diminish, instead of enhance, the (ϕ_{te}/ϕ_{tc}) ratio.

The Excitation Wavelength Effect. Laarhoven and coworkers[16] irradiated *t*-St in CH_3OD and found a significant increase in the carbene insertion/direct addition ratio, ϕ_e^c/ϕ_e^d. on changing λ_{exc}, from 0.6 ± 0.1 at 360 nm to >3 at 185 nm. There was also an increase in the threo/erythro ratio, k_t/k_e, of the 1,2-addition product from 0.7 at 360 nm to 1.8 at 254 nm. Following consideration of alternative mechanisms, they proposed a mechanism involving syn addition of CH_3OD to "planar, unrelaxed $^1(\pi,\pi^*)$ states" of *t*- and *c*-St resulting in threo and erythro ether, respectively, and competing 1,2-addition and carbene formation involving a vibrationally hot twisted diradical excited state.[16]

Selected results for irradiations in CD_3OD from Table S1 are shown in Table 1. They allow evaluation of the λ_{exc} effect on the reactivity of the two isomers separately. Although not in quantitative agreement with the earlier work,[16,17] they confirm the reported trend in the carbene

Table 1. The Excitation Energy Effect on Product Quantum Yields

Starting from	λ_{exc}/nm	ϕ_e^{Total}	ϕ_e^{direct}	$\phi_e^{carbene}$
c-St	313	0.0013	0.00078	0.00053
t-St	313	0.0016	0.0011	0.00049
c-St	254	0.0012	0.00058	0.00057
t-St	254	0.0030	0.0013	0.0017

insertion/direct addition ratio on changing λ_{exc}. Laarhoven and coworkers reported a change in the ϕ_e^c/ϕ_e^d ratio from 0.9 ± 0.3 at 300 nm to 2.0 ± 0.5 at 254 nm. Roberts and Pincock, on the other hand, reported ϕ_e^c/ϕ_e^d = 0.64 at 300 nm.[18] In neither of these studies was the extent of progress to a *cis*-rich quasi-photostationary state considered. In fact the latter value is in good agreement with ϕ_e^c/ϕ_e^d = 0.67 at 313 nm that we observed for *c*-St, Table 1. Our isomer specific GC/MS ratios indicate that at 313 nm the direct addition is favored more starting from *t*-St as would be expected if formation of thermally equilibrated $^1p^*$ from $^1t^*$ underwent less carbene rearrangement. Calculation of partial quantum yields at 313 nm was carried out using the observed GC/MS ratios for the two isomers. For *t*-St we observe a doubling of the ether quantum yield on increasing the excitation energy with most of the increase, a factor of 3.5 (0.00049 at 313 nm and 0.0017 at 254 nm), in the carbene path. Changes for *c*-St are much more modest. The overall ether quantum yields at the two wavelengths are *the same* within experimental error but there is a shift in the partial ether quantum yields in favor of the carbene path at 254 nm. We conclude that following *c*-St excitation at either wavelength, ether formation from both paths involves only the zwitterionic $^1p^*$ intermediate which is not thermally relaxed and whose initial energy increases with increasing excitation energy. At 313 nm in CD_3OD, $(\phi_{te}/\phi_{tc})/(\phi_{ce}/\phi_{ct})$ = 0.86, is very close to the expected α/(1-α) = 0.82 ratio and it follows that $^1p^*$ also accounts for most if not all of the ether formed on excitation of *t*-St at 313 nm. Excess vibrational energy in $^1p^*$favors the carbene pathway and it is likely that the product distribution obtained from $^1t^*$ formed on 313 nm excitation reflects the behavior of vibrationally relaxed $^1p^*$. It is the enhanced ether quantum yields for *t*-St excitation in CD_3OD at 254 nm and Laarhoven's observation of more threo ether in CH_3OD that require the involvement of $^1t^{*\prime}$, a higher *t*-St excited state.

Solvent Deuterium Isotope Effects. Protonation of diphenylcarbene by alcohols was initially proposed by Kirmse based on indirect measurements[70] and later confirmed spectroscopically by the observation of diphenylcarbenium ions.[71-73] Diphenylcarbene has a triplet ground state in aprotic solvents, but in protic solvents strong hydrogen bonding selectively stabilizes the singlet state such that singlet diphenylcarbene is the ground state in the presence of methanol.[74,75]

The deuterium isotope effect on the carbene insertion into OH vs OD, $k_{ec}^{H}/k_{ec}^{D} = 1.4\pm0.2$, determined by Laarhoven and coworkers using a 1:1 CH_3OH/ CH_3OD,[16] is in good agreement with previous measurements for singlet carbene insertion into methanol.[76-80] The $k_{ec}^{H}/k_{ec}^{D} = 1.7$ value determined by Kohler and coworkers by direct transient observation of the 1,1-diphenylmethylcation formed by protonation of singlet diphenylcarbene by methanol[80] is probably the most reliable. It will be used here because, based on the comparison of transient kinetics in the pure CH_3OH and CH_3OD solvents instead of in their 1:1 mixture, it is more relevant to our work.

Laarhoven and coworkers generated the 1-benzyl-1-phenylcarbene by exciting 1,1-diphenylethene in methanol. Formation of 1-methoxy-1,1-diphenylethane, the Markovnikov product, competes with 1,2-phenyl shift, resulting in the same carbene that is obtained from the stilbenes. The carbene gives the expected 1-methoxy-1,2-diphenylethane ether and phenanthrene in a 2:1 ratio. Formation of phenanthrene reveals that carbene insertion into methanol occurs in competition with carbene rearrangement to ground state stilbenes that do not accumulate in more than trace amounts under the reaction conditions.[16] It follows that the carbene reacts with methanol twice as fast as it rearranges, i.e., $k_{ec}/k_{cr} = 2$, where k_{ec} and k_{cr} are the rate constant of the carbene reactions in eqs 13 and 14, respectively. It should be pointed out that Tomioka and coworkers generated the same carbene in CH_3OD by photolysis of 1,2-diphenyldiazoethane.[81]

Ether and the stilbenes formed in 57 and 43% yield, respectively and there was 11% D incorporation in the stilbenes. No D incorporation in the stilbene products was detected by Laarhoven and coworkers.[16]

Relevant results from Table S1 are shown in Table 2. They show that changing the solvent from CH_3OH to CD_3OD diminishes the overall ether quantum yields obtained on 313 nm excitation by factors of 1.4 and 1.8 starting from *c*- and *t*-St, respectively. Use of $k_{ec}^H/k_{ec}^D = 1.7$ and $k_{ec}^H/k_{cr} = 2$ allows calculation of the D isotope effect on the lifetime of the carbene, $\tau_{carb}^H/\tau_{carb}^D = (k_{ec}^D + k_{cr})/(k_{ec}^H + k_{cr}) = 0.72_5$ and on the ratios of ether formation via the carbene

Table 2. The Solvent D-Isotope Effect on Ether Quantum Yields

Starting from	Solvent	ϕ_e^{Total}	ϕ_e^{direct}	$\phi_e^{carbene}$
c-St	CH_3OH	0.0021	0.0011_4	0.0009_3
t-St	CH_3OH	0.0029	0.0018_7	0.0010_3
c-St	CD_3OD	0.0013	0.00078	0.0053
t-St	CD_3OD	0.0016	0.0011	0.00049

and direct pathways, $(\phi_{te}^c/\phi_{te}^d)_H/(\phi_{te}^c/\phi_{te}^d)_D = (k_{ec}^H \tau_{carb}^H/ k_{ec}^D \tau_{carb}^D) = 1.23$. The slower carbene reaction with CD_3OD is partially compensated for by the longer carbene lifetime in that solvent. Applying this ratio on our ratio of ether quantum yields in CD_3OD for *t*-St gives $(\phi_{te}^c/\phi_{te}^d)_H = 0.54_9$ in CH_3OH. The total ether quantum yield for *t*-St in CH_3OH can now be decomposed into the contributions of the two ether pathways: $\phi_{te}^c = 0.010_3$ and $\phi_{te}^d = 0.0018_7$. These values are entered in Tables 1S and 2. It follows that the D isotope effect on the quantum yields for 1,2-addition of methanol starting from *t*-St is $\phi_{te\text{-}H}^d/\phi_{te\text{-}D}^d = 1.7$. At 313 nm the ratio of the quantum

yields for direct CH_3OH and CD_3OD addition to $^1p^*$ is given by eq 24 because we need only consider the first term in eq 22.

$$\frac{\varphi^{\mathrm{d}}_{\text{te-H}}}{\varphi^{\mathrm{d}}_{\text{te-D}}} = \frac{k^{\mathrm{H}}_{\mathrm{tp}}\tau^{\mathrm{H}}_{\mathrm{f}}k^{\mathrm{H}}_{\mathrm{pe}}\tau^{\mathrm{H}}_{\mathrm{p}}}{k^{\mathrm{D}}_{\mathrm{tp}}\tau^{\mathrm{D}}_{\mathrm{f}}k^{\mathrm{D}}_{\mathrm{pe}}\tau^{\mathrm{D}}_{\mathrm{p}}} = \frac{k^{\mathrm{H}}_{\mathrm{pe}}}{k^{\mathrm{D}}_{\mathrm{pe}}} \tag{24}$$

Neglecting solvent effects on the rate of formation of $^1p^*$ and on the lifetimes of $^1t^*$ and $^1p^*$, the quantum yield ratio gives the ratio of the rate constants for direct CH_3OH and CD_3OD addition to $^1p^*$: $k_{\mathrm{pe}}^{\mathrm{H}}/k_{\mathrm{pe}}^{\mathrm{D}} = 1.7$. This D isotope effect is identical to that measured by Kohler and coworkers for protonation of diphenylcarbene in CH_3OH vs CH_3OD, [78] strongly suggesting that $^1p^*$ in the same two solvents also undergoes protonation. The protonation pathway had been disfavored earlier because there was no change in the rate of product formation when the irradiation of *t*-St in CH_3OH was carried out in the presence of 8×10^{-3} M H_2SO_4.[16]

The lifetime of $^1p^*$, τ_{p}, in CH_3OH is not known. The pseudo-unimolecular rate constant for ether formation by direct CH_3OH addition to $^1p^*$, $k_{\text{pe-H}} = 8.3 \times 10^9$ s^{-1}, can be estimated roughly by using $\tau_{\mathrm{p}} = 0.23$ ps. the lifetime of $^1p^*$ in hexane.[7,43] This is an upper limit because the lifetime of $^1p^*$ in CH_3CN, a more polar solvent, is about twice as long as in pentane (see SI in ref 43). Assuming that the quantum yield of ether formation by this pathway is determined by the rate constant of protonation of $^1p^*$, the rate constant of protonation of $^1p^*$ in CH_3OH is more than a factor of 10 slower than the rate constant of diphenylcarbene protonation.[80] Judging from the suppression of the carbene pathway to ether and neglecting solvent effects on the lifetime of $^1p^*$, protonation of $^1p^*$ is 3.3 times faster in CF_3CH_2OH than in CH_3OH.[18]

Intramolecular Deuterium Isotope Effect. Replacement of the vinyl Hs of *t*-St with D affects the ether quantum yields by changing the lifetimes of the excited states and by diminishing the stilbene/carbene rearrangement. Neglecting the involvement of $^1t^{*\prime}$, and using d0 and d2 subscripts to distinguish parameters of undeuterated from those of dideuterated stilbene $(\phi_{te}^{d})_{d0}/(\phi_{te}^{d})_{d2}$, the ratio of the ether quantum yields by direct addition of CH_3OH at 313 nm in eq 25 is based on the first term in eq 22. Relevant ether formation quantum yields from Table S1 are

$$\frac{\varphi_{\mathrm{ted0}}^{\mathrm{d}}}{\varphi_{\mathrm{ted2}}^{\mathrm{d}}} = \frac{k_{\mathrm{tpd0}}\tau_{\mathrm{fd0}}k_{\mathrm{ped0}}\tau_{\mathrm{pd0}}}{k_{\mathrm{tpd2}}\tau_{\mathrm{fd2}}k_{\mathrm{ped2}}\tau_{\mathrm{pd2}}} \tag{25}$$

shown in Table 3. The fluorescence lifetimes of *trans*-α,α′-dideuteriostilbene, *t*-St_{d2}, are known

Table 3. Intramolecular D Isotope Effects on Ether Formation

Starting from	ϕ_e^{Total}	ϕ_e^{direct}	$\phi_e^{carbene}$
t-St_{d0}	0.0029	0.00187	0.00103
t-St_{d2}	0.0058	0.00518	0.00062

to be consistently higher than those of the parent, *t*-St_{d0}, under a variety of conditions.[32] A lifetime increase from 82.9 to 119.2 ps in hexane at 23 °C can be compared with a corresponding change from 42.6 ps for *t*-St_{d0} to 61.1 ps for *t*-St_{d2} in methanol at 24 °C.[32] The increase is a factor of 1.43 in both solvents. Applying this ratio on $\phi_{fd0} = 0.026$ gives $\phi_{fd2} = 0.037$ for *t*-St_{d2}. Although the change in fluorescence quantum yield is significant, their absolute values are small and have a negligible effect on the efficiency of reaching $^1p^*$, $(k_{tpd0}\tau_{fd0})/(k_{tpd2}\tau_{fd2}) = (1-\phi_{fd0})/(1-\phi_{fd2}) = 1.011$. The predicted change is a 1.1% decrease in the population of $^1p^*$ on dideuteration. This small change would not be detected within the experimental error of our ether quantum yield measurements. Protonation of $^1p^*$ involves no hybridization change at the reaction site and,

consequently, the secondary D isotope effect should be negligible, (k_{ped0}/k_{ped2}) = 1. It follows that, with the 1.1% modification, the ratio of the quantum yields for direct ether formation, $\phi_{ted2}\phi_{ted0}$ = 2.7$_7$, gives the ratio of the lifetimes of $^1p^*$, τ_{pd2}/τ_{pd0} = 2.7$_4$. This is in reasonable agreement with the factor of 2 τ_{pd2}/τ_{pd0} ratio estimated in hexane from the quantum yields of $^1t^*$ fluorescence due to the adiabatic $^1c^* \rightarrow {}^1p^* \rightarrow {}^1t^*$ reaction channel.[7]

The ratio of the quantum yields of ether formed by the carbene pathway at 313 nm in eq 26 can be based on the first term in eq 23. With the exceptions of k_{pc}, k_{ec} and τ_{carb}, the effect of D

$$\frac{\varphi^{c}_{ted0}}{\varphi^{c}_{ted2}} = \frac{k_{tpd0}\tau_{fd0}k_{pcd0}\tau_{pd0}k_{ecd0}\tau_{carbd0}}{k_{tpd2}\tau_{fd2}k_{pcd2}\tau_{pd2}k_{ecd2}\tau_{carbd2}} \tag{26}$$

substitution for the vinyl Hs on the parameters in eq 26 is known. The k_{ecdo}/k_{ecd2} ratio of the rate constants for the ether forming reactions, for the undeuterated and dideuterated stilbenes is not expected to deviate from unity because it is only subject to small secondary D isotope effects and the D in the carbene is not at the reaction site. The rate constants for the rearrangements of $^1p^*$ to the carbene, k_{pc}, and of the carbene back to the stilbene, k_r, on the other hand are subject to primary D isotope effects and should decrease significantly on deuteration. Assuming k_{rdo}/k_{rd2} = 6.3, gives $\tau_{carbd0}/\tau_{carbd2}$ = 0.72. Use of our quantum yield ratio for the carbene pathway, $(\phi_{te}^{c})_{d0}/(\phi_{te}^{c})_{d2}$ = 1.66 from Table 3 then gives k_{pcdo}/k_{pcd2} = 6.3. In view of the fact that the two rearrangement reactions involve the same D shifting in opposite directions, it would not be surprising if they experienced similar D isotope effects. However, because the lifetime of the carbene depends primarily on its reaction with methanol, it is rather insensitive to the magnitude of the D isotope effect on the rate constant of its rearrangement. Assuming the extreme case of k_{rd2}/k_{rd0} = 0 gives $\tau_{carbd0}/\tau_{carbd2}$ = 0.67 and results in a minor increase from 6.3 to 6.8 in k_{pcdo}/k_{pcd2}.

CONCLUSIONS

By studying the addition of CH_3OH separately to *c*- and *t*-St we showed that ether formation and cis-trans photoisomerization proceed via torsional relaxation to the common $^1p^*$ twisted intermediate, the phantom singlet state. This short-lived intermediate is common in that it decays predominately to the cis and trans ground state isomers via a zwitterionic conical intersection as predicted by theory[57,58] in a 45/55 decay ratio favoring *c*-St. Inefficient ether formation occurs via protonation of $^1p^*$ and via competing hydride shift to a singlet carbene that also gives ether via protonation. The carbene pathway is favored by higher excitation energy, especially starting from *t*-St, indicating that at least some of the hydride shift occurs in competition with vibronic relaxation of hot $^1p^*$. Protonation of $^1p^*$ in pure methanol is about ten times slower than the extremely fast protonation of singlet diphenylcarbene,[80] whose reactivity, we expect, is similar to that of the singlet benzylphenylcarbene that is involved in our study. The conclusion of Kohler and coworkers that, in pure methanol, solvent reorganization controls the rate of protonation of singlet diphenylcarbene,[80] has received strong recent experimental and theoretical support.[74,75] Not only does the formation of the carbene-methanol hydrogen bonded complex lead to a singlet spin state,[74] but its fate depends on the hydrogen-bonding disposition of nearby methanol molecules.[75] Earlier workers had also proposed differences in reactivity between singlet carbenes and methanol monomers and oligomers.[79,82] We expect similar solvent reorganization considerations to apply to the very fast torsional relaxation and protonation reactions that are described here.

There are strong indications that adduct formation via trapping of the zwitterionic twisted intermediates in alkene photoisomerization is a general reaction. We have already mentioned the addition of ethanol to the DPBs that inspired this work.[19] Noteworthy is also the photohydration

of 3-hydroxystilbene in 1:1 CH_3CN/H_2O.[83] Although a mechanism involving hydration of the trans isomer was proposed, the time evolution of the photoproducts establishes similar reactivity for the two isomers and strongly implicates the common twisted intermediate. Other interesting examples are the photohydrations of *trans*-stilbene, *trans*-3-methoxystilbene and *trans*-3-methoxyanethole in α-, β- and γ-cyclodextrins.[84] Protonation of the excited state by one of the three OH substituents on the rim of the cyclodextrins followed by reaction with H_2O was proposed. The essential role of the cyclodextrin OH was established by the observation that photohydration is completely suppressed when trimethyl-β-cyclodextrin was employed.[84] The photoaddition of CH_3OH to 2-(3-aminostyryl)naphthalene[85] and the photohydrations of 1- and 2-(3-hydroxystyryl)naphthalenes[86] are other potential candidates for $^1p^*$ involvement in adduct formation. Photochemical addition of the NH bond of secondary alkylamines across the central bond of stilbenes also occurs both inter-[87] and intra-molecularly.[88] Protonation by the neutral amine is not an attractive initial step and a strong case has been made for its occurrence as a second step following formation of the stilbene anion radical by electron transfer. However, the fact that *t*- and *c*-St undergo intramolecular photoaddition at similar rates[88] does suggest that $^1p^*$ can serve as a stilbene partner in these reactions also.

SUPPORTING INFORMATION

Table S1 listing all quantum yields measured in this work. This material is available free of charge via the Internet at http://pubs.acs.org.

AUTHOR INFORMATION

Corresponding Author

*Email: saltiel@chem.fsu.edu

The authors declare no competing financial interests.

ACKNOWLEDGMENT

This research was supported in part by the National Science Foundation, most recently by Grant No. CHE-1361962. It was also supported by the Florida State University. We thank Mr. David Boose for technical assistance in initial experiments.

REFERENCES

(1) Saltiel, J.; Charlton, J. L. Cis-Trans Isomerization of Olefins. In *Rearrangements in Ground and Excited States*; de Mayo, P. Ed.; Academic Press: New York, 1980, Vol III, pp 25-89.

(2) Saltiel, J.; Sun, Y.-P. Cis-Trans Isomerization of C=C Double Bonds. In *Photochromism, Molecules and Systems*; Dürr, H. and Bouas-Laurent, H., Eds.; Elsevier: Amsterdam, 1990; pp 64-164.

(3) Waldeck, D. H. Photoisomerization Dynamics of Stilbenes. *Chem. Rev.* **1991**, *91*, 415-436.

(4) Saltiel, J.; Sun, Y.-P. The Intrinsic Potential Energy Barrier for Twisting in the trans-Stilbene S_1 State in Hydrocarbon Solvents. *J. Phys. Chem.* **1989**, *93*, 6246-6250.

(5) Saltiel, J.; Waller, A. S.; Sears, Jr., D. F.; Garrett, C. Z. Fluorescence Quantum Yields of *trans*-Stilbene-d_0 and -d_2 in *n*-Hexane and *n*-Tetradecane. Medium and Deuterium Isotope Effects on Decay Processes. *J. Phys. Chem.* **1993**, *97*, 2516-2522.

(6) Saltiel, J.; Waller, A. S.; Sears, Jr., D. F.; Hoburg, E. A.; Zeglinski, D. M.; Waldeck, D. H. Fluorescence Quantum Yields and Lifetimes of Substituted Stilbenes in *n*-Alkanes. A

Rexamination of the Relationship between Solute Size and Medium Effect on Torsional Relaxation. *J. Phys. Chem.* **1994**, *98*, 10689-10698.

(7) Saltiel, J.; Waller, A. S.; Sears, Jr., D. F. The Temperature and Medium Dependencies of *cis*-Stilbene Fluorescence. The Energetics for Twisting in the Lowest Excited Singlet State. *J. Am. Chem. Soc.* **1993**, *115*, 2453-2465.

(8) Saltiel, J. Perdeuteriostilbene. The Role of Phantom States in the Cis-Trans Photoisomerization of Stilbenes. *J. Am. Chem. Soc.* **1967**, *89*, 1036-1037.

(9) Saltiel, J. Perdeuteriostilbene. The Triplet and Singlet Paths for Stilbene Photoisomerization. *J. Am. Chem. Soc.* **1968**, *90*, 6394-6400.

(10) Saltiel, J.; Waller, A.; Sun, Y.-P.; Sears, Jr., D. F. *cis*-Stilbene Fluorescence in Solution. Adiabatic ^{1}c* to ^{1}t* Conversion. *J. Am. Chem. Soc.* **1990**, *112*, 4580-4581.

(11) Saltiel, J.; A. S. Waller, A. S.; Sears, Jr., D. F. Dynamics of *cis*-Stilbene Photoisomerization: The Adiabatic Pathway to Excited *trans*-Stilbene. *J. Photochem. Photobiol. A: Chem.* **1992**, *65*, 29-40.

(12) Moore, W. M.; Morgan, D. D.; Stermitz, F. R. The Photochemical Conversion of Stilbene to Phenanthrene. The Nature of the Intermediate. *J. Am. Chem. Soc.* **1963**, *85*, 829-830.

(13) Muszkat, K. A. The 4a,4b-dihydrophenanthrenes. *Topics Curr. Chem.* **1890**, *88*, 89-144.

(14) Mallory, F. B.; Mallory, C. W. Photocyclization of Stilbenes and Related Molecules. *Org. React.* **1984**, *30*, 1-456.

(15) Laarhoven, W. H. 4n + 2 Systems: Molecules Derived from *Z*-hexa-1,3.5-triene/cyclohexa-1,3-diene. In Photochromism, Molecules and Systems, Diirr, H., Bouas-Laurent, H., Eds., Elsevier: Amsterdam, 1990, pp 270-3 13.

(16) Woning, J.; Oudenampsen, A.; Laarhoven, W. H. Photochemical Addition of Methanol to Stilbenes. *J. C. S. Perkin Trans. 2* **1989**, 2147-2154.

(17) Roberts, J. C.; Pincock, J. A. The Photochemical Addition of 2,2,2-Trifluorethanol to Methoxy-Substituted Stilbenes. *J. Org. Chem.* **2004**, *69*, 4279-4282.

(18) Roberts, J. C.; Pincock, J. A. Methoxy-substituted Stilbenes, Styrenes, and 1-arylpropenes: Photophysical Properties and Photoadditions of Alcohols. *J. Org. Chem.* **2006**, *71*, 1480-1492.

(19) Saltiel, J.; Redwood, C. E. Photochemistry of the 1,4-Diphenyl-1,3-butadienes in Ethanol. Trapping Conical Intersections. *J. Phys. Chem. A* **2016**, *120*, 2832-2840.

(20) Saltiel, J.; Marinari, A.; Chang, D. W.-L.; Mitchener, J. C.; Megarity, E. D. Trans-Cis Photoisomerization of the Stilbenes and a Reexamination of the Positional Dependence of the Heavy-Atom Effect. *J. Am. Chem. Soc*. **1979,** *101*, 2982-2996.

(21) Moses, F. G.; Liu, R. S. H.; Monroe, B. M. The "Merry-Go-Round" Quantum Yield Apparatus. *Mol. Photochem.* **1969**, *1*, 245-249.

(22) Gegiou, D.; Muszkat, K. A.; Fischer, E. Temperature Dependence of Photoisomerization. VI. The Viscosity effect. *J. Am. Chem. Soc.* **1968**, *90*, 12 -18.

(23) Rodier, J.-M.; Myers, A. *cis*-Stilbene Photochemistry: Solvent Dependence of the Initial Dynamics and Quantum Yields. *J. Am. Chem. Soc.* **1993**, *115*, 10791-10795.

(24) Sundström, V.; Gillbro, T. Dynamics of the Isomerization of *Trans*-stilbene in *n*-alcohols by Ultraviolet Picosecond Absorption Recovery. *Chem. Phys. Lett.* **1984**, *109*, 538-543.

(25) Saltiel, J.; Rousseau, A. D.; Sykes, A. Temperature and Viscosity Effects on the Decay Characteristics of *s-trans*-1,3-Diene Triplets. *J. Am. Chem. Soc.* **1972**, *94*, 5903-5905.

(26) Saltiel, J.; Ganapathy, S.; Werking, C. The ΔH for Thermal Trans/Cis Stilbene Isomerization. Do S_0 and T_1 Potential Energy Curves Cross? *J. Phys. Chem.* **1987,** *91*, 2755-2758.

(27) Dietz, W. A. Response Factors for Gas Chromatographic Analyses. *J. Gas Chromatogr.* **1967**, *5*, 68-71.

(28) Luan, F.; Liu, H. T.; Wen, Y.; Zhang, X. Prediction of Quantitative Calibration Factors of Some Organic Compounds in Gas Chromatography. *Analyst* **2008**. *133*, 881-887.

(29) Lamola, A. A.; G. S. Hammond, G. S. Intersystem Crossing Efficiencies. *J. Chem. Phys.* **1965,** *43*, 2129-2135.

(30) Kropp, P. J. Photorearrangement and Fragmentation of Alkenes. In *CRC Handbook of Photochemistry and Photobiology*; Horspool, W., Lenci, F., Eds.; CRC Press: Boca Raton, 2004; pp 13-1-13-15.

(31) Catalán, J.; Saltiel, J. On the Origin of Nonvertical Triplet Excitation Transfer. The Relative Role of Double-Bond and Phenyl-Vinyl Torsions in the Stilbenes. *J. Phys. Chem. A* **2001,** *105*, 6273-6276.

(32) Courtney, S. H.; Balk, M. W.; Philips L. A.; Webb, S. P.; Yang, D.; Levy, D. H.; Fleming, G. R. Unimolecular Reactions in Isolated and Collisional Systems – Deuterium Isotope Effect in the Photoisomerization of Stilbene. *J. Chem. Phys.* **1988**, *89*, 6697-6707.

(33) Kim, S. K.; Courtney, S. H.; Fleming, G. R. Isomerization of *trans*-Stilbene in Alcohols. *Chem. Phys. Lett.* **1989**, *159*, 543-548.

(34) Abrash, S.; Repinec, S.; Hochstrasser, R. M. The Viscosity Dependence and Reaction Coordinate for Isomerization of *cis*-Stilbene. *J. Chem. Phys.* **1990**, *93*, 1041-1053.

(35) Rice, J. K.; Baronavski, A. P. Ultrafast Studies of Solvent Effects in the Isomerization of *cis*-Stilbene. *J. Phys. Chem.* **1992, *96***, 3359-3366.

(36) Nikowa, L.; Schwarzer, D.; Troe, J.; Schroeder, J. Viscosity and Solvent Dependence of Low-barrier Processes: Photoisomerization of *cis*-stilbene in Compressed Liquid Solvents. *J. Chem. Phys.* **1992**, *97*, 4827-4835.

(37) Sension, R, J.; Repinec, S. T.; Szarka, A. Z.; Hochstrasser, R. M. Femtosecond Laser Studies of the *cis*-stilbene Photoisomerization Reactions. *J. Chem. Phys.* **1993**, *98*. 269-279.

(38) Todd, D. C.; Fleming, G. R. *cis*-Stilbene Isomerization: Temperature Dependence and the Role of Mechanical Friction. *J. Chem. Phys.* **1993**, *98*, 269-279.

(39) Ishii, K.; Takeuchi, S.; Tahara, T. A 40-fs Time-resolved Absorption Study on *cis*-stilbene in Solution: Observation of Wavepacket Motion on the Reactive Excited State. *Chem. Phys. Lett.* **2004**, *398*, 400-406.

(40) Hicks, J. M.; Vandersall, M. T.; Sitzman, E. V.; Eisenthal, K. B. Polarity Dependent Barriers and the Photoisomerization Dynamics of Molecules in Solution. *Chem. Phys. Lett.* **1987**, *135*, 413-420.

(41) Zwier, T. S. The Spectroscopy of Solvation in Hydrogen-Bonded Aromatic Clusters. *Annu. Rev. Phys. Chem.* **1996**. *47*, 205–241.

(42) Pribble, R. N.; Hagemeister, F. C.; Zwier, T. S. Resonant Ion-dip Infrared Spectroscopy of Benzene–(methanol)$_m$ Clusters with m = 1–6. *J. Chem. Phys*. **1997**, *106*, 2145-2157.

(43) Kovalenko, S. A.; Dobrayakov, A. L.; Ioffe, I.; Ernsting, N. P. Evidence for the Phantom State in Photoinduced Cis-trans Isomerization of Stilbene. *Chem Phys Lett.* **2010**, *493*, 255-258.

(44) Moore, W. M.; Morgan, D. D.; Stermitz, F. R. The Photochemical Conversion of Stilbene to Phenanthrene. The Nature of the Intermediate. *J. Am. Chem. Soc.* **1963**, *85*, 829-830.

(45) Hammond, G. S.; Saltiel, J.; Lamola, A. A.; Turro, N. J.; Bradshaw, J. S.; Cowan, D. O.; Counsell, R. C.; Vogt, V; Dalton, C. Photochemical Cis-Trans Isomerization. *J. Am. Chem. Soc.* **1964**, *86*, 3197-3217.

(46) Saltiel, J. Photoisomerization of the Stilbenes: An Application of Chemical Spectroscopy, *Ph. D. Dissertation* California Institute of Technology, Pasadena, CA 1964, p.46.

(47) Muszkat, K. A.; Fischer, E. Structure, Spectra, Photochemistry, and Thermal Reactions of the 4a,4b-Dihydrophenanthrenes. *J. Chem. Soc. B* **1967**, 662-678.

(48) Quick, M.; Berndt, F.; Dobryakov, A. L.; Ioffe, I. N.; Granovsky, A. A.; Knie, C.; Mahrwald, R.; Lenoir, D.; Ernsting, N. P.; Kovalenko, S. A. Photoisomerization Dynamics of Stiff-Stilbene in Solution. *J. Phys. Chem. B* **2014**, *118*, 1389-1402.

(49) Nakamura, T.; Takeuchi, S.; Taketsugu, T.; Tahara, T. Femtosecond Fluorescence Study of the Reaction Pathways and Nature of the Reactive S_1 State of *Cis*-stilbene. *Phys. Chem. Chem. Phys.* **2012**, *14*, 6225–6232.

(50) Dauben, W. G.; Ritscher, J. S. Photochemistry of Ethylidenecyclooctenes. Mechanism of Bicyclobutane Formation. *J. Am. Chem. Soc.* **1970**, *92*, 2925-2926.

(51) Dauben, W. G.; Wipke, W. T. Photochemistry of Dienes. *Pure Appl. Chem.* **1964**, *9*, 539-533.

(52) Dauben, W, G.; Wipke, W. T. Nuclear Magnetic Resonance Spectra of Bicyclo[n.1.0]alkane Derivatives. *J. Org. Chem.* **1967**, *32*, 2976–2980.

(53) Salem, L. The Sudden Polarization Effect and Its Possible Role in Vision. *Acc. Chem. Res.* **1979**, *12*, 87-92.

(54) Michl, J. Photochemical Reactions of Large Molecules. I. A Simple Physical Model of Photochemical Reactivity. *Mol. Photochem.* **1972**, *4*, 243-255.

(55) Michl, J. Photochemical Reactions of Large Molecules. II. Application of the Model to Organic Photochemistry. *Mol. Photochem.* **1972**, *4*, 257-286.

(56) Yarkony, D. R. Conical Intersections: Diabolical and Often Misunderstood. *Acc. Chem. Res.* **1998**, *31*, 511-518.

(57) Levine, B. G.; Martínez, T. J. Isomerization Through Conical Intersections. *Annu. Rev. Phys. Chem.* **2007**, *58*, 613-634.

(58) Quenneville, J.; Martínez, T. J. Ab Initio Study of Cis-Trans Photoisomerization in Stilbene and Ethylene. *J. Phys. Chem. A* **2003,** *107,* 829-837.

(59) Minezawa, N.; Gordon, M. S. Photoisomerization of Stilbene: A Spin-Flip Density Functional Theory Approach. *J. Phys. Chem. A* **2011**, *115*, 7901–7911.

(60) Ioffe, I. N.; Granovsky, A. A.; Photoisomerization of Stilbene: The Detailed XMCQDPT2 Treatment. *J. Chem. Theory Comput.* **2013**, *9*, 4973−4990.

(61) Tomasello, G.; Garavelli, M.; Orlandi, G. Tracking the Stilbene Photoisomerization in the S_1 State Using RASSCF. *Phys.Chem. Chem.Phys.* **2013**, *15*, 19763-19773.

(62) Harabuchi, Y.; Keipert, K.; Zahariev, F.; Taketsugu, T.; Gordon, M. S. Dynamics Simulations with Spin-Flip Time-Dependent Density Functional Theory: Photoisomerization and Photocyclization Mechanisms of *cis*-Stilbene in $\pi\pi^*$ States. *J. Phys. Chem. A* **2014**, *118*, 11987-11998.

(63) Squillacote, M.; Wang, J.; Chen, J. Electrostatic Control of the Regioselectivity in the Photoisomerization of *trans,trans*-1-Fluoro-2,4-hexadiene: Evidence for Competing Conical Intersections. *J. Am. Chem. Soc.* **2004**, *126*, 1940-1941.

(64) Redwood, C.; Kumar, R. V. K.; Hutchinson, S. Mallory, F. B.; Mallory, C. W.; Clark, R. J. Dmitrenko, O.; Saltiel, J. Photoisomerization of *cis*-1,2-di(1-methyl-2-naphthyl)ethene at 77 K in glassy media. *Photochem. Photobiol.* **2015**, *91*, 607-615.

(65) Saltiel, J.; Ko, D.-H.; Fleming, S. A. Differential Medium Effects on the Trans to Cis Photoisomerization of all-trans-1,6-Diphenyl-1,3,5-hexatriene. Competing Diradicaloid vs Zwitterionic Pathways. *J. Am. Chem. Soc.* **1994**, *116*, 4099-4100.

(66) Saltiel, J.; Wang, S.; Watkins, L. P.; Ko, D.-H. Direct Photoisomerization of the 1,6-Diphenyl-1,3,5-hexatrienes. Medium Effect on Triplet and Singlet Contributions. *J. Phys. Chem. A* **2000**, *104*, 11443-11450.

(67) Wismontski-Knittel, T.; Fischer, G.; Fischer, E. Temperature Dependence of Photoisomerization. Part VIII Excited-state Behaviour of 1-Naphthyl-2-phenyl- and 1,2-Dinaphthyl-ethylenes and their Photocyclisation Products, and Properties of the Latter. *J. Chem. Soc., Perkin Trans. 2* **1974**, 1930-1940.

(68) Repinec, S. T.; Sension, R. J.; Szarka, A. Z.; Hochstrasser, R. M. Femtosecond Laser Studies of the *cis*-Stilbene Photoisomerization Reactions. The *cis*-Stilbene to Dihydrophenanthrene Reaction. *J. Phys. Chem.* **1991**, *95*, 10380-10385.

(69) Petek, H.; Yoshihara, K.; Fujiwara, Y,; Lin, Z.; Penn, J. H.; Frederick, J. H. Is the Nonradiative Decay of S_1 *cis*-Stilbene Due to the Dihydrophenanthrene Isomerization Channel? Suggestive Evidence from Photophysical Measurements on 1,2-Dlphenylcycloaikenes. *J. Phys. Chem.* **1990**, *94*, 1539-1543.

(70) Kirmse, W. Nucleophils Verhalten des Diphenylcarbens. *Justus Liebigs Ann. Chem.* **1963**, *666*, 9-.

(71) Kirmse, W.; Kilian, J.; Steenken, S. Carbenes and the OH Bond: Spectroscopic Evidence for Protonation of Diarylcarbenes to Give Diarylcarbenium Ions. *J. Am. Chem. Soc.* **1990**, *112*, 6399-6400.

(72) Chateauneuf, J. E. Picosecond Spectroscopic Detection of Diphenylcarbenium Ion in the Photolysis of Diphenyldiazomethane in Aliphatic Alcohols. *JCS Chem. Commun.* **1991**, 1437-1438.

(73) Simon, T. B.; Bohne, C.; Charette, G.; Sugamori, S. E.; Scaiano, J. C. Carbocation Formation via Carbene Protonation Studied by the Technique of Stopped-Flow Laser-Flash Photolysis. *J. Am. Chem. Soc.* **1993**, *115*, 2200-2205.

(74) Costa, P.; Sander, W. Hydrogen Bonding Switches the Spin State of Diphenylcarbene from Triplet to Singlet. *Angew. Chem. Int. Ed.* **2014**, *53*, 5122 –5125.

(75) Knorr, J.; Sokkar, P.; Schott, S.; Costa, P.; Thiel, W.; Sander, S. Sanchez-Garcia, E.; Nuernberger, P. Competitive Solvent-molecule Interactions Govern Primary Processes of Diphenylcarbene in Solvent Mixtures. *Nature Comm.* **2016**, *7*, 1-8.

(76) Bethell, D.; Newall, A. R.; Whittaker, D. Intermediates in the Decomposition of Aliphatic Diazo Compounds. The Mechanism of Ether Formation from Diarylmethylenes and Alcohols *J. Chem. Soc. B* **1971**, 23-31.

(77) Zupancic, J. J.; Grasse, P. B.; Lapin S. C.; Schuster, G. B. The Reactions of Fluorenylidene with Heteroatomic Nucleophiles. *Tetrahedron* **1985**, *41*, 1471-1478.

(78) Turro, N. J.; Cha, Y.; Gould, I. R. Temperature Dependence of the Reactions of Singlet and Triplet Diphenylcarbene: Evidence for Reversible Ylide Formation in the Reaction with Alcohols. *Tetrrahedron Lett.* **1985**, *26*, 5951-5954.

(79) Dix, E. J.; Goodman, J. L. Protonation of Diarylcarbenes by Alcohols: The Importance of Ion Pair Dynamics. *J. Phys. Chem.* **1994**, *98*, 12609-12612.

(80) Peon, J.; Polshakov, D.; Kohler, B. Solvent Reorganization Controls the Rate of Proton Transfer from Neat Alcohol Solvents to Singlet Diphenylcarbene. *J. Am. Chem. Soc.* **2002**, *124*, 6428-6438.

(81)Tomioka, H.; Hayashi, N.; Sugiura, T.; Izawa, Y. Evidence for Protonation of Typically Electrophilic Carbenes by Methanol. *J. C. S. Chem. Comm.* **1986**, 1364-1366.

(82) Griller, D.; Liu, M. T. H.; Scaiano, J. C. Hydrogen Bonding in Alcohols: Its Effect on the Carbene Insertion Reaction. *J. Am. Chem. Soc.* **1982**, *104*, 5549-5551.

(83) Murohoshi, T.; Kaneda, K.; Ikegami, I.; Arai, T. Photoisomerization and isomer-specific addition of water in hydroxystilbenes. *Photochem. Photobiol. Sci.* **2003**, *2*, 1247–1249.

(84) Suresh, P.; Pitchumani, K. Novel Photohydration of *Trans*-stilbenes and *Trans*-anethole Inside Cyclodextrin Nanocavity in Aqueous Medium *J. Photochem. Photobiol. A: Chem.* **2009**, *206*, 40–45.

(85) Lewis, F. D.; Yang, J.-S. The Excited State Behavior of Aminostilbenes. A New Example of the Meta Effect. *J. Am. Chem. Soc.* **1997**, *119*, 3834–35.

(86) Bandini, E.; Bortolus, P.; Manet, I.; Monti, S.; Galliazzo, G.; Gennari, G. Photoisomerization and Photohydration of 3-hydroxystyrylnaphthalenes. *Photochem. Photobiol. Sci.* **2005**, *4*, 862-868.

(87) Lewis, F. D.; Ho, T.-I. *trans*-Stilbene-Amine Exciplexes. Photochemical Addition of Secondary and Tertiary Amines to Stilbene. *J. Am. Chem. Soc.* **1977**, *99*, 7991-7996.

(88) Lewis, F. D; Bassani, D. M.; Burch, E. L.; Cohen, B. E.; Engleman, J. A.; Reddy, G. D.; Schneider, S.; Jaeger, W.; Gedeck, P.; Gahr, M. Photophysics and Photochemistry of Intramolecular Stilbene-Amine Exciplexes. *J. Am. Chem. Soc.* **1995**, *117*, 660-669.

TOC GRAPHICS